

## Test for Interlayer Coherence in a Quasi-Two-Dimensional Superconductor

John Singleton,<sup>1,2</sup> P. A. Goddard,<sup>2</sup> A. Ardavan,<sup>2</sup> N. Harrison,<sup>1</sup> S. J. Blundell,<sup>2</sup> J. A. Schlueter,<sup>3</sup> and A. M. Kini<sup>3</sup>

<sup>1</sup>National High Magnetic Field Laboratory, LANL, MS-E536, Los Alamos, New Mexico 87545

<sup>2</sup>Department of Physics, University of Oxford, Clarendon Laboratory, Parks Road, Oxford OX1 3PU, United Kingdom

<sup>3</sup>Materials Science Division, Argonne National Laboratory, Argonne, Illinois 60439

(Received 30 April 2001; published 2 January 2002)

Peaks in the magnetoresistivity of the layered superconductor  $\kappa - (\text{BEDT-TTF})_2\text{Cu}(\text{NCS})_2$ , measured in fields  $\leq 45$  T applied within the layers, show that the Fermi surface is extended in the interlayer direction and enable the interlayer transfer integral ( $t_{\perp} \approx 0.04$  meV) to be deduced. However, the quasiparticle scattering rate  $\tau^{-1}$  is such that  $\hbar/\tau \sim 6t_{\perp}$ , implying that  $\kappa - (\text{BEDT-TTF})_2\text{Cu}(\text{NCS})_2$  meets the criterion used to identify interlayer incoherence. The applicability of this criterion to anisotropic materials is thus shown to be questionable.

DOI: 10.1103/PhysRevLett.88.037001

PACS numbers: 74.70.Kn, 71.20.Rv, 78.20.Ls

Many interesting correlated-electron systems have a very anisotropic electronic band structure. Examples include the “high- $T_c$ ” cuprates [1,2], layered ruthenates [3], and crystalline organic metals [2,4]. Such systems may be described by a tight-binding Hamiltonian in which the ratio of the interlayer transfer integral  $t_{\perp}$  to the average intralayer transfer integral  $t_{\parallel}$  is  $\ll 1$  [2,4,5]. The inequality  $\hbar/\tau > t_{\perp}$  [6], where  $\tau^{-1}$  is the quasiparticle scattering rate [1,2,5], often applies to such systems, suggesting that the quasiparticles scatter more frequently than they tunnel between layers. It is thus natural to consider whether the interlayer charge transfer is coherent or incoherent, i.e., whether or not the Fermi surface (FS) extends in the interlayer direction [2,4,5]. In this paper we have used magnetoresistance data to estimate the interlayer transfer integral in the highly anisotropic organic superconductor  $\kappa - (\text{BEDT-TTF})_2\text{Cu}(\text{NCS})_2$ . We find that  $\hbar/\tau \approx 6t_{\perp}$ . Nevertheless, our data demonstrate a FS which is extended in the interlayer direction.

$\kappa - (\text{BEDT-TTF})_2\text{Cu}(\text{NCS})_2$  was selected for our experiments because it is perhaps the most thoroughly characterized quasi-two-dimensional (Q2D) conductor [4]. The FS topology is well known from Shubnikov-de Haas (SdH) and de Haas-van Alphen (dHvA) studies [4] and from angle-dependent magnetoresistance oscillation (AMRO) [7] and millimeter-wave (MMW) experiments [8]; it consists of a pair of quasi-one-dimensional (Q1D) electron sheets plus a Q2D hole pocket (see Fig. 1a [9,10]). Optical data on the  $\kappa$ -phase BEDT-TTF salts may be interpreted as consistent with interlayer incoherence [11]. Moreover, models for superconductivity in  $\kappa$ -phase BEDT-TTF salts invoke the nesting properties of the FS [10,12,13]; the degree of nesting might depend on whether the FS is a 2D or a 3D entity (see [4], Sect. 3.5). Experimental tests for coherence in  $\kappa - (\text{BEDT-TTF})_2\text{Cu}(\text{NCS})_2$  are thus far deemed to be inconclusive [5]; e.g., semiclassical models can reproduce AMRO [7] and MMW data [8] equally well when the interlayer transport is coherent or “weakly coherent” [5].

To examine how interlayer coherence might be detected, we use a tight-binding dispersion relationship  $-2t_{\perp} \cos(k_{\perp}a)$  to represent the interlayer dispersion, where  $k_{\perp}$  is the interlayer component of  $\mathbf{k}$  and  $a$  is the interlayer spacing. This is added to the *effective dimer model*, which is known to represent the *intralayer* band structure accurately [9,10], to yield

$$E(\mathbf{k}) = \pm 2 \cos\left(\frac{k_b b}{2}\right) \sqrt{t_{c1}^2 + t_{c2}^2 + 2t_{c1}t_{c2} \cos(k_c c)} + 2t_b \cos(k_b b) - 2t_{\perp} \cos(k_{\perp} a). \quad (1)$$

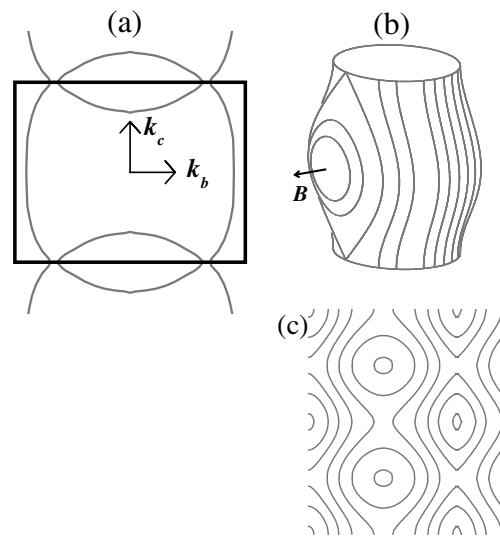


FIG. 1. (a) Cross section of the Fermi surface (FS) and Brillouin zone of  $\kappa - (\text{BEDT-TTF})_2\text{Cu}(\text{NCS})_2$  predicted by Eq. (1) [10,11]. (b) Perspective view of the Q2D FS section described by Eq. (1); the intralayer curvature and interplane warping have been exaggerated for clarity. The lines indicate quasiparticle orbits on the FS due to the in-plane field  $\mathbf{B}$ . Note the closed orbits about the “belly” of the FS. (c) Plan view of closed orbits about the Q1D FS section caused by  $\mathbf{B}$  applied parallel to  $\mathbf{k}_b$ . Two families of closed orbits are possible; one on the flatter portions of the Q1D FS, roughly parallel to  $\mathbf{k}_c$ , and the second around the more highly curved region at the zone boundary.

Here  $k_b$  and  $k_c$  are the intralayer components of  $\mathbf{k}$  (see Fig. 1a) and  $t_b$ ,  $t_{c1}$ , and  $t_{c2}$  are interdimer transfer integrals [9,10]; the + and - signs result in the Q1D sheets and Q2D pocket of the FS, respectively (Fig. 1a). The addition of the interlayer dispersion produces a warping of *both* Q2D and Q1D FS sections. This is shown schematically for the Q2D section in Fig. 1b; the FS cross section is modulated in the interlayer direction. This modulation might suggest that separate “neck and belly” frequencies would be observed in the dHvA effect [4]; however, only a single frequency is seen in low-field studies [14], suggesting that the cyclotron energy exceeds  $t_\perp$  at the fields at which quantum oscillations are observed.

Therefore, in view of the inconclusive nature of other tests [5], we have chosen to examine the behavior of  $\kappa$ -(BEDT-TTF)<sub>2</sub>Cu(NCS)<sub>2</sub> in almost exactly in-plane magnetic fields [5,15,16]. The motion of quasiparticles of charge  $q$  in a magnetic field  $\mathbf{B}$  is determined by the Lorentz force  $\hbar\mathbf{k} = q\mathbf{v} \times \mathbf{B}$ , where the quasiparticle velocity is given by  $\hbar\mathbf{v} = \nabla_{\mathbf{k}}E$  [17]; this leads to orbits on the FS in planes perpendicular to  $\mathbf{B}$ . Hence, if the FS is extended in the interlayer direction, an in-plane field will cause closed orbits on the bellies (see Fig. 1b). Such orbits are effective at averaging  $v_\perp$ , the interlayer component of the velocity, and their presence will lead to an increase in the magnetoresistivity component  $\rho_{zz}$  [15,16].  $\mathbf{B}$  can then be tilted away from the in-plane direction by an angle  $\Delta$ , such that the small closed orbits about the bellies cease to be possible; this occurs when  $\mathbf{B}$  is parallel to  $\mathbf{v}$  at the point at which  $v_\perp$  is a maximum. Therefore, on tilting  $\mathbf{B}$  around the in-plane orientation, we expect to see a peak in  $\rho_{zz}$ , of angular width  $2\Delta$ , if (and only if [5]) the FS is extended in the interlayer direction.

A complication occurs for  $\mathbf{B}$  almost parallel to  $\mathbf{k}_b$  (Fig. 1a), when two families of closed orbits will be possible on the warped Q1D FS sections (Fig. 1c). At such orientations, we expect three separate contributions (one from the Q2D FS section, and two from the Q1D sections) of different angular width to the peak in  $\rho_{zz}$ .

A problem in using  $\kappa$ -(BEDT-TTF)<sub>2</sub>Cu(NCS)<sub>2</sub> is its high in-plane critical field;  $\mu_0 H_{c2}(T=0) \approx 35$  T, falling to  $\mu_0 H_{c2} \approx 25$  T at 4.2 K [18]. Moreover, apparent peaks in the resistivity of  $\kappa$ -(BEDT-TTF)<sub>2</sub>Cu(NCS)<sub>2</sub> in in-plane fields may occur due to dissipative processes associated with vortices within the mixed state [4,19]. To ensure that such effects do not interfere, we choose to stay at fields well above the superconducting state; hence, data were recorded in the 45 T hybrid magnet at NHMFL in Tallahassee. The experiments involved two single crystals ( $\sim 0.7 \times 0.5 \times 0.1$  mm<sup>3</sup>; mosaic spread  $\leq 0.1^\circ$ ) of  $\kappa$ -(BEDT-TTF)<sub>2</sub>Cu(NCS)<sub>2</sub>, made using electrocrystallization [20]. In one, the terminal hydrogens of BEDT-TTF were isotopically substituted by deuterium; we refer to this crystal as *d8*, and the hydrogenated sample as *h8* [21]. Both crystals were mounted in a <sup>3</sup>He cryostat which allowed rotation to all possible orientations in  $\mathbf{B}$  [18]; sample

orientation is defined by the angle  $\theta$  between  $\mathbf{B}$  and the normal to the sample’s Q2D planes and the azimuthal angle  $\phi$  ( $\phi = 0$  is a plane of rotation of  $\mathbf{B}$  containing  $\mathbf{k}_b$  and the normal to the Q2D planes). The interlayer magnetoresistance  $R_{zz}$  ( $\propto \rho_{zz}$ ) was measured using four-terminal ac techniques [18].

Figure 2 shows  $R_{zz}$  of the *d8* sample close to the in-plane orientation  $\theta = 90^\circ$ ; data for three values of  $\phi$  are shown. (The data for the *h8* sample were very similar in all respects [21].) The edges of Fig. 2 are dominated by AMROs and related phenomena; as these are well known [5,22] in  $\kappa$ -(BEDT-TTF)<sub>2</sub>Cu(NCS)<sub>2</sub> [7], we shall not describe them further in this paper. Close to  $\theta = 90^\circ$ , there is a distinct peak in  $R_{zz}$ , the width and height of which vary with  $\phi$ ; we attribute this peak to the closed orbits described above.

Figure 3 shows the peak at temperatures  $T$  from 0.48 to 5.1 K; increasing  $T$  by over an order of magnitude reduces the peak height but has little effect on its width. Varying the field (in the range 35–45 T at 0.5 K, and in the range 29–45 T at 4.2 K) also has little effect on the peak width; increases of field result in increases in peak height and definition, in a manner similar to the field dependence of AMROs [4]. Both of these observations support the idea that the peak is a consequence of the FS geometry alone.

Figure 4 shows the variation of  $2\Delta$ , the full width of the peak close to  $\theta = 90^\circ$  versus  $\phi$ ; the width was deduced

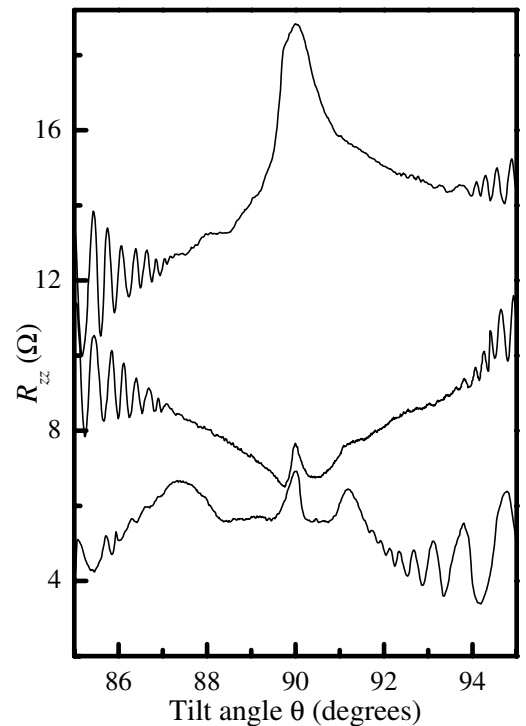


FIG. 2. Interlayer resistance  $R_{zz}$  for the *d8*  $\kappa$ -(BEDT-TTF)<sub>2</sub>Cu(NCS)<sub>2</sub> sample as a function of tilt angle  $\theta$ . Data for three planes of rotation of the field are shown:  $\phi = 25^\circ$  (upper),  $\phi = 20^\circ$  (middle), and  $\phi = 15^\circ$  (lower). The static magnetic field is 42 T, and the temperature is 520 mK.

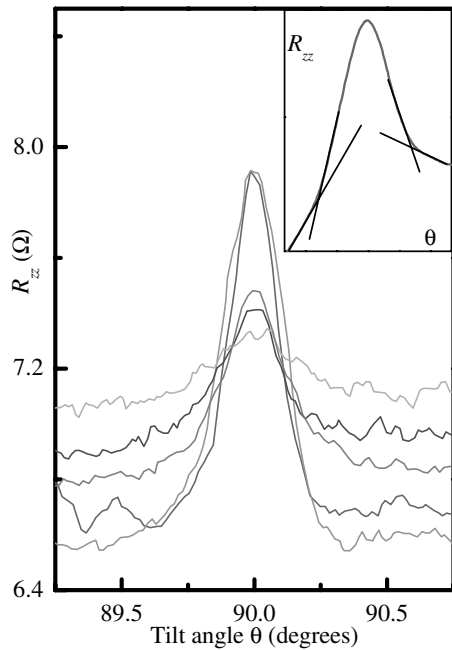


FIG. 3. Interlayer resistance ( $R_{zz}$ ) versus angle  $\theta$  for temperatures  $T = 0.48, 1.4, 3.0, 4.4,$  and  $5.1$  K ( $\phi = 135^\circ$ ). The background magnetoresistance increases with increasing  $T$ , whereas the peak at  $\theta = 90^\circ$  becomes smaller. The data shown are for the  $d8$   $\kappa$ -(BEDT-TTF) $_2$ Cu(NCS) $_2$  sample. The inset shows the intersections of the linear extrapolations used to determine the peak width.

using the extrapolations shown in Fig. 3 (inset). In order to interpret this variation, we use Eq. (1) to calculate  $v_{\perp \max}$ , the maximum value of  $v_{\perp}$ , and  $v_{\parallel}$ , the intralayer velocity component parallel to the plane of rotation of  $\mathbf{B}$ ; when measured in radians,  $\Delta \approx v_{\perp \max}/v_{\parallel}$ . As all of the relevant quasiparticle motion occurs close to the Fermi energy,  $E \approx E_F$ , we adjust the parameters of Eq. (1) to reproduce the known FS parameters of  $\kappa$ -(BEDT-TTF) $_2$ Cu(NCS) $_2$ . First,  $t_c/t_b$  (where  $t_c$  is the mean of  $t_{c1}$  and  $t_{c2}$ ) is adjusted to obtain the dHvA frequencies of the Q2D pocket and the magnetic breakdown orbit [9,21,23]. The absolute value of  $t_c$  is then constrained by fitting to the effective mass of the breakdown orbit [4,21]. Third, the energy gap measured in magnetic breakdown ( $E_g \approx 7.8$  meV [23]) gives  $t_{c1} - t_{c2} = E_g/2$  [9], leading to  $t_b = 15.6$  meV,  $t_{c1} = 24.2$  meV, and  $t_{c2} = 20.3$  meV. Finally,  $a = 16.2$  Å [20], so that equations for  $\Delta$  contain only one adjustable parameter,  $t_{\perp}$ . The substitution of  $t_{\perp} = 0.04$  meV leads to the curves shown in Fig. 4; the continuous curve is from the Q2D FS, and the loops are caused by the Q1D sheets, which support closed orbits only over a restricted range of  $\phi$ . In the latter case, the lower branch of the loop results from the flatter portions of the Q1D FS, roughly parallel to  $\mathbf{k}_c$ ; the upper branch is due to the more highly curved region at the zone boundary (Figs. 1a and 1c).

For most  $\phi$ , there is agreement between curve and data (Fig. 4), but around  $\phi = 0$  and  $180^\circ$  it seems that the observed peak width is sometimes dominated by closed orbits

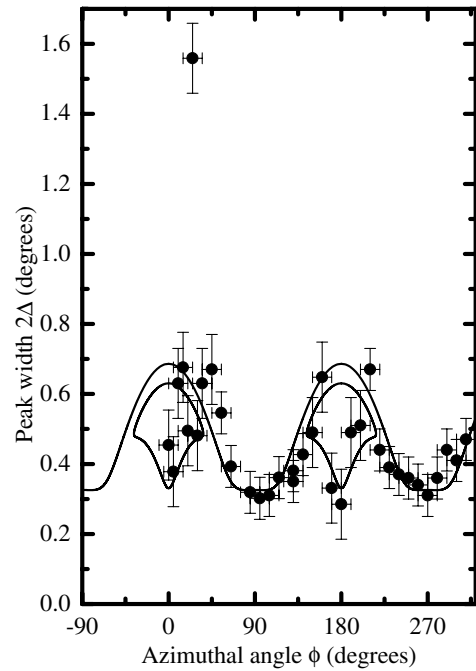


FIG. 4. Angular width  $2\Delta$  of peak in  $R_{zz}$  ( $B = 42$  T,  $T \approx 500$  mK) versus azimuthal angle  $\phi$ ; data for the  $d8$   $\kappa$ -(BEDT-TTF) $_2$ Cu(NCS) $_2$  sample are shown. Points are data; the curves represent the model prediction with  $t_{\perp} = 0.04$  meV. The continuous curve is due to the Q2D FS section; the Q1D sheets can support closed orbits over a restricted range of  $\phi$ , leading to the top-shaped loops.

on the Q1D sheets, and sometimes by those on the Q2D FS section; the dominant width presumably depends on which section of the FS able to support closed orbits (Figs. 1b and 1c) is the most effective at averaging  $v_{\perp}$  [24]. MMW studies [8] suggest that the interlayer corrugations of the Q1D sheets are slightly more complex than those given by Eq. (1), and this could lead to a rapid variation with  $\phi$  of the effectiveness of the various orbits in increasing  $\rho_{zz}$ . For a narrow range of angles close to  $\phi = 25^\circ$ , the peak was particularly wide and large (see top trace, Fig. 2). This is perhaps connected to the gap between the Q1D and Q2D FS sections.

As mentioned above, the band structure of  $\kappa$ -(BEDT-TTF) $_2$ Cu(NCS) $_2$  within the Q2D layers is determined by the interdimer transfer integrals [9,10]. A better guide to the *total* intralayer bandwidth than the parameters used above (relevant for  $E \approx E_F$  and thus including renormalizing interactions [4,9]) is given by the fits to optical data of Ref. [9], which suggest  $t_b \approx 60$  meV and  $t_c \approx 120$  meV; these are a factor  $\approx 10^3$  larger than  $t_{\perp} \approx 0.04$  meV.

The failure of the dHvA effect [14] to observe necks and bellies may now be understood; the Landau-level spacing at the lowest  $|\mathbf{B}|$  used ( $\sim 6$  T) is  $0.2$  meV,  $\sim 5t_{\perp}$ .

Let us now compare  $t_{\perp}$  with  $\tau^{-1}$ . Samples  $d8$  and  $h8$  have been studied using SdH oscillations at  $|\mathbf{B}| \leq 15$  T [22]. At such fields, the 2D form of the

Lifshitz-Kosevich formula may be used to extract  $\tau$  [4], giving  $\tau = 2.9 \pm 0.5$  ps ( $h8$ ) and  $\tau = 2.6 \pm 0.3$  ps ( $d8$ ) [22]. Another estimate can be derived from MMW studies [8], which measure the FS-traversal resonance (FTR) due to quasiparticles crossing the Q1D FS sheets; these experiments used samples from the same batch as  $h8$ . In the data of [8], the FTR appears at  $B \approx 10$  T, with a full width at half maximum of  $\Delta B \approx 7$  T. If we assume that  $\omega\tau \sim B/\Delta B$  [25], where  $\omega = 2\pi \times 70 \times 10^9$  rad s $^{-1}$  [8], we obtain  $\tau \sim 3$  ps, close to the SdH values [26]. Thus,  $\hbar/\tau \approx 0.24$  meV,  $\sim 6t_{\perp}$ . In spite of this, the peak in  $\rho_{zz}$  described above unambiguously demonstrates a 3D FS topology.

The criterion for incoherent transport was developed for isotropic disordered metals [27]; the mean-free path  $\lambda$  was taken to represent the spatial extent over which the Bloch waves are coherent and is, by default, isotropic. However, in Q2D systems  $\lambda_{\parallel} \gg \lambda_{\perp}$  [26], so that a purely ballistic model of transport [27] fails to preserve information on the spatial extent of the wave functions in the interlayer direction. Our experiment therefore demonstrates inadequacies in such models. When impurities are randomly dispersed, the interimpurity separation should be almost isotropic. Hence, we should expect the spatial coherence of the Bloch states to be roughly isotropic, even when the group velocity is highly anisotropic.

Finally, the data in Fig. 3 show that the signature of the 3D FS persists up to temperatures  $k_B T \approx 10t_{\perp}$ . This observation also calls into question the assertion that interlayer transport is incoherent if  $k_B T > t_{\perp}$  [28].

In summary, we observe a peak in the interlayer resistance of the highly anisotropic superconductor  $\kappa$ -(BEDT-TTF) $_2$ Cu(NCS) $_2$  when a magnetic field is applied within the layers. This demonstrates [5] that the Fermi surface is extended in the interlayer direction, and allows the interlayer transfer integral to be estimated to be  $t_{\perp} \approx 0.04$  meV ( $t_{\perp}/k_B \approx 0.5$  K). We find that  $\kappa$ -(BEDT-TTF) $_2$ Cu(NCS) $_2$  obeys the criterion commonly used to delineate interlayer incoherence— $\hbar/\tau \geq t_{\perp}$ —and yet it clearly possesses a three-dimensional Fermi surface, even when  $k_B T \approx 10t_{\perp}$  [28]. It is perhaps now time to reexamine the validity of such criteria when applied to strongly anisotropic systems.

This work is supported by EPSRC (U.K.). NHMFL is supported by the U.S. Department of Energy (DoE), the National Science Foundation, and the State of Florida. Work at Argonne is sponsored by the DoE, Office of Basic Energy Sciences, Division of Materials Science under Contract No. W-31-109-ENG-38. We thank Vic Emery and Jane Symington for stimulating discussions.

[1] L. B. Ioffe and A. J. Millis, *Science* **285**, 1241 (2000).

- [2] D. G. Clarke and S. P. Strong, *Adv. Phys.* **46**, 545 (1997).  
 [3] C. Bergemann *et al.*, *Phys. Rev. Lett.* **84**, 2662 (2000).  
 [4] J. Singleton, *Rep. Prog. Phys.* **63**, 1111 (2000).  
 [5] R. H. McKenzie and P. Moses, *Phys. Rev. Lett.* **81**, 4492 (1998); *Phys. Rev. B* **60**, 11 241 (1999).  
 [6] This is roughly equivalent to the Mott-Ioffe-Regel criterion [7]; see, e.g., [5] or section 7.2 of [2].  
 [7] M. S. Nam *et al.*, *Synth. Met.* **103**, 1905 (1999).  
 [8] J. M. Schrama *et al.*, *J. Phys. Condens. Matter* **13**, 2235 (2001).  
 [9] J. M. Caulfield *et al.*, *J. Phys. Condens. Matter* **6**, 2911 (1994).  
 [10] Jörg Schmalian, *Phys. Rev. Lett.* **81**, 4232 (1998).  
 [11] J. J. McGuire *et al.*, *cond-mat/0103237*.  
 [12] R. Louati *et al.*, *Synth. Met.* **103**, 1857 (1999).  
 [13] K. Kuroki and H. Aoki, *Phys. Rev. B* **60**, 3060 (1999).  
 [14] T. Sasaki *et al.*, *Phys. Rev. B* **57**, 10 889 (1998).  
 [15] T. Osada *et al.*, *Phys. Rev. Lett.* **77**, 5261 (1996); N. Hanasaki *et al.*, *Phys. Rev. B* **57**, 1336 (1998); **60**, 11 210 (1999).  
 [16] Others propose that self-crossing orbits (SCOs) are more effective than closed orbits in averaging  $v_{\perp}$ . However, the geometrical constraints on the peak in  $\rho_{zz}$  are identical for closed orbits and SCOs if the in-plane dispersion relationship is parabolic [see V. G. Peschansky and M. V. Kartsovnik, *Phys. Rev. B* **60**, 11 207 (1999); I. J. Lee and M. J. Naughton, *Phys. Rev. B* **57**, 7423 (1998)]. It is straightforward to show that the bands predicted by Eq. (1) are almost parabolic at  $E \approx E_F$ .  
 [17] N. W. Ashcroft and N. D. Mermin, *Solid State Physics* (Saunders, Philadelphia, 1976).  
 [18] J. Singleton *et al.*, *J. Phys. Condens. Matter* **12**, L641 (2000).  
 [19] M. Chaparala *et al.*, *Phys. Rev. B* **53**, 5818 (1996).  
 [20] H. Uryama *et al.*, *Chem. Lett.* **1988**, 463 (1988).  
 [21] AMRO and SdH data [23] show that  $d8$  and  $h8$  have very similar FSs; e.g., the SdH frequency and effective mass of the Q2D pocket in  $d8$  ( $h8$ ) are  $597 \pm 1$  T ( $600 \pm 1$  T) and  $(3.4 \pm 0.1)m_e$  [ $(3.5 \pm 0.1)m_e$ ] [23]. The only marked difference is that the magnetic breakdown probability is somewhat higher in  $d8$  [23].  
 [22] P. A. Goddard *et al.* (to be published).  
 [23] N. Harrison *et al.*, *J. Phys. Condens. Matter* **8**, 5415 (1996).  
 [24] See e.g., M. V. Kartsovnik *et al.*, *J. Phys. I (France)* **2**, 89 (1992).  
 [25] For example, B. I. Bleaney and B. Bleaney, *Electricity and Magnetism* (Oxford University Press, New York, 1990), p. 734.  
 [26]  $\tau \approx 3$  ps gives an intralayer mean-free path  $\lambda_{\parallel} = v_{\parallel}\tau \approx 0.2$   $\mu\text{m}$ . By contrast, the same figure gives an interlayer mean-free path  $\lambda_{\perp} \sim \bar{v}_{\perp}\tau \approx 3$   $\text{\AA}$ . Mean-free path formalism implies that only  $\sim \exp(-16.2/3) \approx 0.5\%$  of the quasiparticles travel between adjacent layers (separation 16.2  $\text{\AA}$  [15]) without scattering.  
 [27] N. F. Mott and E. H. Davies, *Electronic Properties of Non-crystalline Materials* (Taylor and Francis, London, 1975); A. F. Ioffe and A. R. Regel, *Prog. Semicond.* **4**, 237 (1960).  
 [28] P. W. Anderson, *The Theory of Superconductivity in the High  $T_c$  Cuprates* (Princeton University Press, Princeton, NJ, 1997), p. 50.